

## CHAPTER II



## LITERATURE REVIEW

### 1. Botanical aspects of *Plumbago indica* Linn.

*Plumbago indica* Linn. (syn. *Plumbago rosea* L.) (Figure 2) or rose-colored leadwort (common name) or Chetta mun phloeng daeng (Thai name) belongs to the family Plumbaginaceae (คณะเภสัชศาสตร์ มหาวิทยาลัยมหิดล, 2535; นันทวัน บุญยะประกาศ และอรนุช ไชคชัยเจริญพร, 2539; เต็ม สมิตินันท์, 2544). The name "*plumbago*" is derived from the Latin *plumbum* which means "lead", since the plant was supposed to be a cure for lead poisoning (Hyam and Pankhurst, 1995).

*P. indica* has been distributed in the tropical region, especially in the South-East Asia (Hyam and Pankhurst, 1995). This plant is a perennial sub-scandent shrub, 0.8-1.5 m high, with semi-woody striated stems and flexible branches (Figure 2A). The leaves are simple, alternate, oblong, 3-5 cm wide, 6-10 cm long (Figure 2B). The flowers are bright red, in long terminal spike. The calyx ribs are covered with sessile glands (Figure 2C). The red corolla is slender; its tubes are longer than the calyx. The fruits are circumscissile capsules at the base, the caduceous part often splitting towards the apex. (คณะเภสัชศาสตร์ มหาวิทยาลัยมหิดล, 2535; นันทวัน บุญยะประกาศ และอรนุช ไชคชัยเจริญพร, 2539; Kubitzki, Rohwer and Bittrich, 1993).

### 2. Uses of *Plumbago indica* Linn.

Thomson (1971) has reported that *Plumbago* roots have been credited with some remarkable powers. It can stain the skin and produce blisters. In France, the

root is believed to be effective for relieving tooth-ache and, in Malaysia, it is used to produce abortion. In India, where the root is known as Chita or Chitraka, the crude drug has been reported to be useful in dyspepsia, piles, anasarca, diarrhea and skin diseases (Thomson, 1971). In Thai folk medicine, the dried roots (Figure 2D) have been used as emmenagogue, stomachic, carminative and treatment of hemorrhoid. Plumbagin was shown to cause uterus and intestinal stimulation and act as gastric acid inducer to promote the appetite. However, it was also cause gastrointestinal irritation and might be toxic (คณะเภสัชศาสตร์ มหาวิทยาลัยมหิดล, 2535).

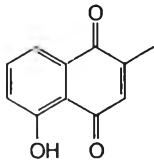
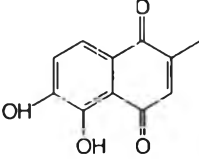
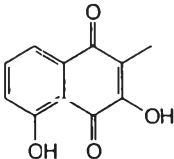
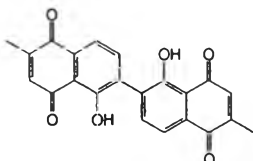
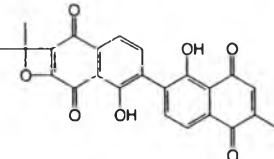
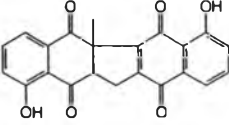


**Figure 2** *Plumbago indica* Linn. (Plumbaginaceae). A: whole plant, B: young shoot, C: flower and D: dried root.

### 3. Chemical constituents of *Plumbago indica* Linn.

*Plumbago indica* Linn. has been reported to contain several groups of natural products, including flavonoids, tannins, sterols and naphthoquinones. Flavonoids have been found in its leaves and flowers, for example, leucodelphinidin was found in the leaves, whereas delphinidin, cyanidin and pelargonidin 3-rhamnoside and kaempferol 3-rhamnoside were found in the flowers (Harborne, 1967). Sterols (sitosterol, stigmasterol and campesterol) and plumbaginol have been isolated from the aerial part of this plant (Dinda and Chel, 1992; Dinda, Chel and Achari, 1994). It has been reported that the naphthoquinone plumbagin occurs mainly in the root tissues (Harborne, 1967). Plumbagin and its structurally related compounds have also been found in this plant and its *in vitro* cultures as listed in Table 1.

**Table 1** Plumbagin and its structurally related compounds reported to be present in *Plumbago indica* Linn.

Compound name	Chemical structure	Plant part	Reference
Plumbagin		Aerial part, root, root bark, micropropagated plant, callus culture, cell suspension culture and root culture	Harborne, 1967; Dinda and Chel, 1992; Komaraiah et al., 2002; 2003a; 2003b; Panichayupakaranant and Tewtrakul, 2002; Satheeshkumar and Seeni, 2003
6-Hydroxyplumbagin		Aerial part	Dinda and Chel, 1992
Droserone		Root	Dinda, Das and Hajra, 1995
Elliptinone		Root	Dinda et al., 1995
Roseanone		Root	Dinda et al., 1995
Zeylanone		Root	Dinda et al., 1995

## 4. Plumbagin

### 4.1 Structure and chemical properties

Plumbagin (Figure 3) is a natural naphthoquinone present in the roots and aerial parts of *P. indica* (Harborne, 1967; Dinda and Chel, 1992). Its chemical name is 5-hydroxy-2-methyl-1,4-naphthoquinone. It has a formula of  $C_{11}H_8O_3$  with a molecular mass of 188.17.

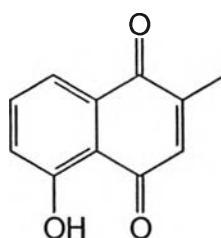


**Figure 3** The chemical structure of plumbagin

Plumbagin occurs as yellow needles. Its melting point is 78-79 °C. It is slightly soluble in hot water and soluble well in alcohol, acetone, chloroform, benzene and acetic acid (Budavari, et al., 1989).

For physical properties of plumbagin, its ultraviolet spectrum shows  $\lambda_{\max}$  (ethanol) at 220, 266, 418 nm (log  $\epsilon$  3.87, 4.12, 3.61).  $\lambda_{\max}$  (KBr) at 1659, 1637, 1602  $\text{cm}^{-1}$ . The mass spectrum (EIMS)  $m/z$  (rel. int.): 189 ( $[M+H]^+$ , 14), 188 (100), 173 (20.5), 160 (17), 145 (3), 132 (9.5), 131 (14), 121 (8.5), 120 (14), 92 (13), 77 (5), 64 (5.5), 63 (9), 51 (5) (Fallas and Thomson, 1968; Thomson, 1971).

### 4.2 Distribution of plumbagin-containing plants

Plumbagin is a natural yellow pigment found in the plants of Plumbaginaceae, Droseraceae, Drosophyllaceae, Ebenaceae, Nepenthaceae and Ancistrocladaceae as summarized in Table 2.

**Table 2** Occurrence of plumbagin in the plant kingdom.

Plant	Thai name	Plant part	Reference
<b>Family Plumbaginaceae</b>			
<i>Plumbago auriculata</i> Lam. (syn. <i>P. capensis</i> Thunb.)	เจตมูลเพลิงฝรั่ง	Root	Harborne, 1967; Van Der Vijver and Lötter, 1971
<i>Plumbago coerulea</i> Kunth	-	Leaf, flower and root	Harborne, 1967
<i>Plumbago europaea</i> L.	-	Leaf, flower and root	Harborne, 1967
<i>Plumbago indica</i> L. (syn. <i>P. rosea</i> L.)	เจตมูลเพลิงแดง	Aerial part, root	Harborne, 1967; Dinda and Chel; 1972
<i>Plumbago pearsonii</i> L. Bolus	-	Root	Van Der Vijver, 1972
<i>Plumbago scandens</i> L.	-	Leaf and root	Harborne, 1967
<i>Plumbago zeylanica</i> L.	เจตมูลเพลิงขาว	Root, micropropagated plant, hairy root culture	Harborne, 1967; Van Der Vijver and Lötter, 1971; Verma et al., 2002
<i>Ceratostigma minus</i> Stapf ex Prain	-	Whole plant	Yue et al., 1994
<i>Ceratostigma willmottianum</i> Stapf	-	Whole plant	Yue et al., 1997

Table 2 (continued)

Plant	Thai name	Plant part	Reference
<b>Family Droseraceae</b>			
<i>Drosera anglica</i> Huds. ( <i>Drosera longifolia</i> L.)	-	Leaf and whole plant	Bendz and Lindberg, 1968; Zenk et al., 1969
<i>Drosera auriculata</i> Planch.	-	Leaf	Zenk et al., 1969
<i>Drosera binata</i> Labill.	-	Leaf	Zenk et al., 1969
<i>Drosera capensis</i> L.	-	Leaf	Zenk et al., 1969
<i>Drosera cistiflora</i> L.	-	Leaf	Zenk et al., 1969
<i>Drosera dichotoma</i> Smith	-	Leaf	Zenk et al., 1969
<i>Drosera gigantea</i> Lindl.	-	<i>In vitro</i> culture	Budzianowski, 2000
<i>Drosera indica</i> L.	หญ้าน้ำค้าง	Leaf	Zenk et al., 1969
<i>Drosera intermedia</i> Hayne	-	Whole plant and <i>in vitro</i> culture	Bendz and Lindberg, 1968; Budzianowski, 1996
<i>Drosera lunata</i> D.C.	-	Leaf	Zenk et al., 1969
<i>Drosera ramentacea</i> Burch.	-	Whole plant	Krishnamoorthy and Thomson, 1969
<i>Drosera rotundifolia</i> L.	-	<i>In vitro</i> culture	Budzianowski, 1996
<i>Drosera whittakeri</i> Planch.	-	Leaf	Zenk et al., 1969
<i>Dionaea muscipula</i> Ellis	-	Whole plant and leaf	Zenk et al., 1969; Kreher, Neszmélyi and Wagner, 1990

Table 2 (continued)

Plant	Thai name	Plant part	Reference
<b>Family Drosophyllaceae</b>			
<i>Drosophyllum lusitanicum</i> Link.	-	Leaf and cell suspension culture	Zenk et al., 1969 ; Nahálka et al., 1996
<b>Family Ebenaceae</b>			
<i>Diospyros canaliculata</i> De Wild	-	Stem bark	Zhong, Waterman and Jeffreys, 1984 ; Mallavadhani et al., 1998
<i>Diospyros elliptifolia</i> Merr.	-	Stem bark	Fallas and Thomson, 1968; Mallavadhani et al., 1998
<i>Diospyros hebecarpa</i> A. Cunn.	-	Leaf and fruit	Cooke and Dowd, 1952; Mallavadhani et al., 1998
<i>Diospyros kaki</i> L.	พลับจัน	Root	Tezuka et al., 1973; Mallavadhani et al., 1998
<i>Diospyros maritima</i> Blume	-	Fruit and root	Tezuka et al., 1973; Kuo et al., 1997; Higa, Ogihara and Yogi, 1998; Mallavadhani et al., 1998.
<i>Diospyros olen</i> Hiern	-	Stem bark	Evans et al., 1999

Table 2 (continued)

Plant	Thai name	Plant part	Reference
<i>Diospyros siamang</i> Bakh.	-	Stem bark and wood	Zakaria et al., 1984; Mallavadhani et al., 1998
<i>Diospyros walkeri</i> Guerke	-	Bark	Herath et al., 1978; Mallavadhani et al., 1998
<i>Diospyros wallichii</i> Williams	ดำตะโก	Stem bark and wood	Zakaria et al., 1984; Mallavadhani et al., 1998
<b>Family Nepenthaceae</b>			
<i>Nepenthes gracilis</i> Korth.	-	Leaf	Aung et al., 2002
<i>Nepenthes rafflesiana</i> Jack.	-	Root	Cannon et al., 1980
<i>Nepenthes thorelii</i> Lec.	น้ำเต้าลม	Root	Likhitwitayawuid et al., 1998
<b>Family</b>			
<b>Ancistrocladaceae</b>			
<i>Ancistrocladus</i> <i>cochinchinensis</i> Gagnep.	ลั่นทรวง	Leaf	Anh et al., 1997
<i>Ancistrocladus heyneanus</i> Wall. ex J. Grah.	-	<i>In vitro</i> culture	Bringmann et al., 1999

### 4.3 Biological activities of plumbagin

Plumbagin is a natural naphthoquinone showing a broad range of bioactivities. It has been reported to manifest significant abortifacient activity in the albino rats without any teratogenic effect after giving orally (1 and 2 mg/100 g) (Premakumari, Rathinam and Santhakumari, 1977). In dog given a dose of 10 mg/kg *i.p.* for 60 days, plumbagin caused selective testicular lesions. The wet weight of testes and epididymides was found to decrease. It has been shown to cause reduction in the diameter of seminiferous tubules and leydig cells nuclei, as well as drastic curtailment in cellular heights of epididymides. Significant reduction in protein RNA and sialic acid concentration was also observed, while the intratesticular cholesterol and acid/alkaline phosphatase was found to be raised after drug treatment (Bhargava, 1984). Plumbagin has been studied for its effect on cell growth and mitosis in chick embryo fibroblast cultures (Santhakumari, Saralamma and Radhakrishnan, 1980). At lower concentration, it behaved like a spindle poison by inhibiting cell mitosis. It exhibited mimetic, nucleotoxic and cytotoxic effects (Santhakumari et al., 1980). Plumbagin also exerted various biological activities against microorganisms, for example *Candida albicans*, *Escherichia coli*, *Peptostreptococcus constellatus*, *Prevotella* spp. and *Staphylococcus* spp. (Durga, Sridhar and Polasa, 1990; Didry et al., 1994; Ribeiro de Paiva et al., 2003). It has also been found to have anticancer (Fujii et al., 1992; Parimala and Sachdanandam, 1993; Kuo et al., 1997; Lin et al., 2003), antimalarial activity (Likhitwitayawuid et al., 1998) and anticoagulant activities (Santhakumari, Rathinam, and Seshadri, 1978). Plumbagin was also shown to inhibit insect development, presumably by interfering with hormonal processes of moulting (Kubo et al., 1983; Mitchell and Smith, 1988; Gujar, 1990) and therefore, it might be used for insect killing in agriculture.

#### 4.4 Biosynthesis of plumbagin

Plumbagin biosynthesis has been demonstrated by feeding experiments to *Plumbago europaea* (Durand and Zenk, 1971) and cell cultures of *Ancistrocladus heyneanus* (Bringmann et al., 1998; Bringmann and Feineis, 2001). It has been suggested that plumbagin is formed by the well-known polyketide pathway. The biosynthetic pathway of plumbagin has been proposed as shown in Figure 1. Acetyl-CoA is first condensed with five acetyl residues derived from malonyl-CoA to form a hexaketide intermediate via condensation reaction. The folding of this intermediate molecule can lead to plumbagin. (Durand and Zenk, 1971; Bringmann et al., 1998; Bringmann and Feineis, 2001).

#### 5. Plant polyketide synthases

Polyketide synthases (PKS) catalyze the biosynthesis of structurally diverse natural products in plants, fungi, and bacteria (Schröder, 1997; Shen, 2003). These natural products exhibit different biological and pharmacological properties, including antimicrobial, immunosuppressant, and anticancer activities. A PKS generates a polyketide chain from simple molecular building blocks, such as acetate and propionate units, by catalyzing a series of decarboxylative condensation reactions. The amazing structural diversity of these molecules results from varying the length and constituents of the polyketide and through the enzymes that modify the final scaffold (Jez et al., 2001). Three types of PKSs are known. In plants, polyketides are synthesized by type III PKSs or chalcone synthase-like PKS enzymes (Schröder, 2000; Austin and Noel, 2003).

Type III PKSs are structurally and mechanistically the simplest PKS functioning as a homodimeric iterative PKS (monomer  $M_r \cong 42\text{--}45$  kDa) with two independent



active sites that catalyze a series of decarboxylation, condensation, and cyclization reactions (Schröder, 1997; Shen, 2003; Austin and Noel, 2003).

Plant type III PKS or the family of chalcone synthase (CHS)-related enzymes can produce various types of compounds based on their functional diversity such as substrate specificities, condensation reactions, types of ring closure of the release products, and in some cases by modification of reaction intermediates by additional enzymes (Schröder, 2000). The reactions leading to various diversified products of known plant type III polyketide synthases are shown in Figure 4.

### 5.1 Chalcone synthase (CHS)

Chalcone synthase (CHS) was the first type III PKS enzyme to be discovered. The first demonstration of CHS activity *in vitro* was reported in 1972 with extracts from parsley (*Petroselinum crispum*) cell suspension cultures (Kreuzaler and Hahlbrock, 1972). The enzyme catalyzes the formation of the flavanone naringenin from *p*-coumaroyl-CoA and malonyl-CoA. CHS catalyzes the sequential decarboxylative addition of three acetate units from malonyl-CoA to a *p*-coumaroyl-CoA starter molecule derived from phenylalanine *via* the general phenylpropanoid pathway. In the same active site, CHS then forms 4,2',4',6'-tetrahydrochalcone (chalcone) *via* the intramolecular cyclization and aromatization of the resulting linear phenylpropanoid tetraketide (Kreuzaler and Hahlbrock, 1975) (Figure 5). Thus, CHS catalyzes the first committed step of multi-branched flavonoid pathway and it is important to flavonoid biosynthesis in plants. After the first isolation of a *chs* gene in 1983 (Reimold et al., 1983), until March 2002, nearly 650 *chs*-like gene sequences have been found in gymnosperms and angiosperms (Austin and Noel, 2003).

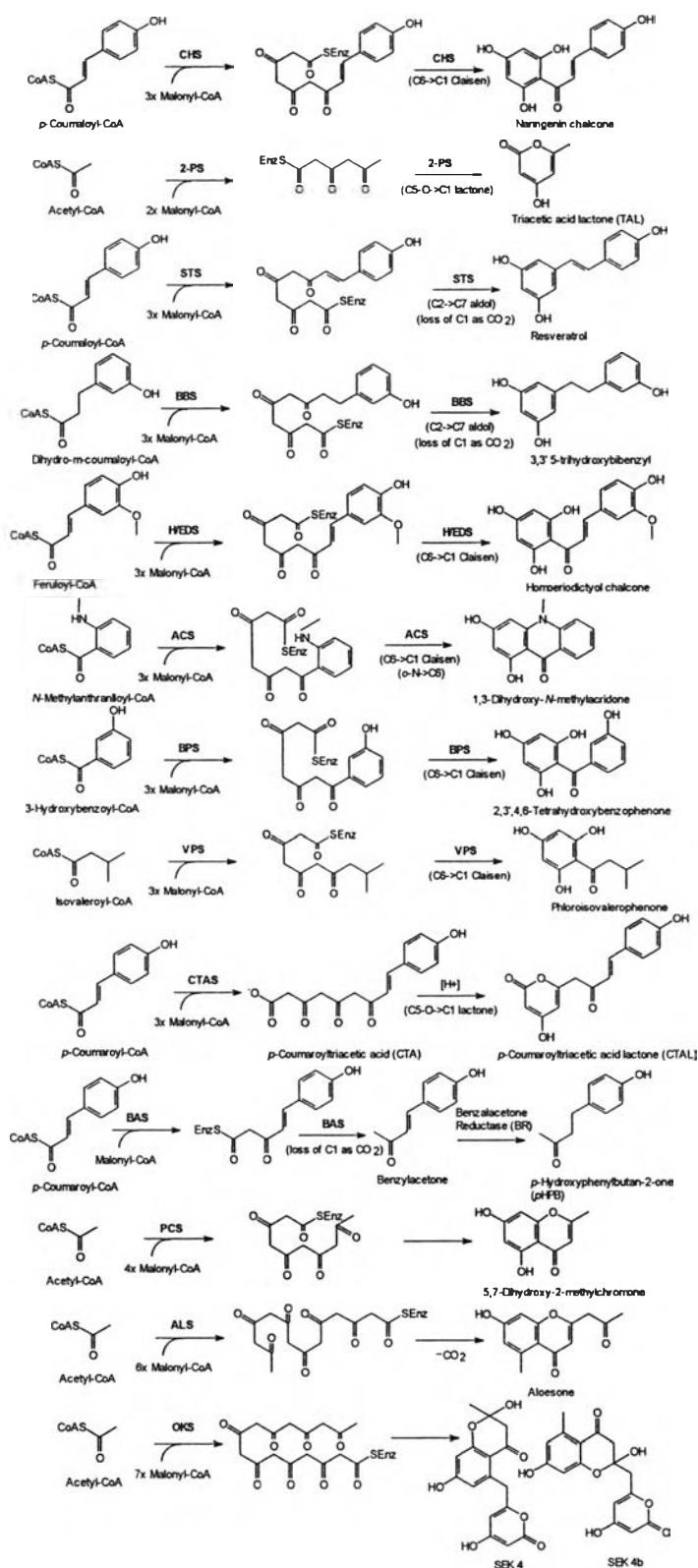


**Figure 4** Comparison of the reactions and products of known divergent plant type III polyketide synthases. The position and type of cyclization reaction (Claisen, aldol, or lactone) of each presumed linear polyketide intermediate is depicted.

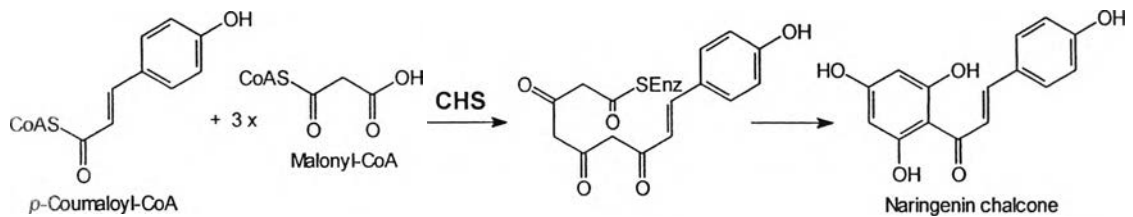


**Figure 5** The formation of naringenin-chalcone from *p*-coumaroyl-CoA and malonyl-CoA by chalcone synthase (CHS).

### 5.1.1 CHS structure

Structure and function of CHS have been studied in *Medicago sativa* (alfalfa) since 1999 (Ferrer et al., 1999). CHS functions as a homodimer of two 42 kDa polypeptides. Structurally, the CHS enzyme forms a symmetric dimer with each monomer related by a two-fold crystallographic axis (Figure 6A). The dimer interface is a fairly flat surface delineated by two structural features. First, the N-terminal  $\alpha$ -helix of monomer A entwines with the corresponding  $\alpha$ -helix of monomer B. Second, a tight loop containing a *cis*-peptide bond between Met137 and Pro138 exposes the methionine side chain as a knob on the monomer surface. Across the interface, Met137 protrudes into a hole found in the surface of the adjoining monomer to form part of the active site cavity. Thus, dimerization forms the complete CHS active site. Structures of CHS complexes with different coenzyme A (CoA) thioesters and product analogs (i.e., naringenin and resveratrol) show that the active site is buried within an interior cavity located at the cleft between the upper and lower domains of each monomer. Considering the complexity of the reaction mechanism leading to chalcone formation, there are remarkably few chemically reactive amino acids in the active site. In particular, four residues conserved in the

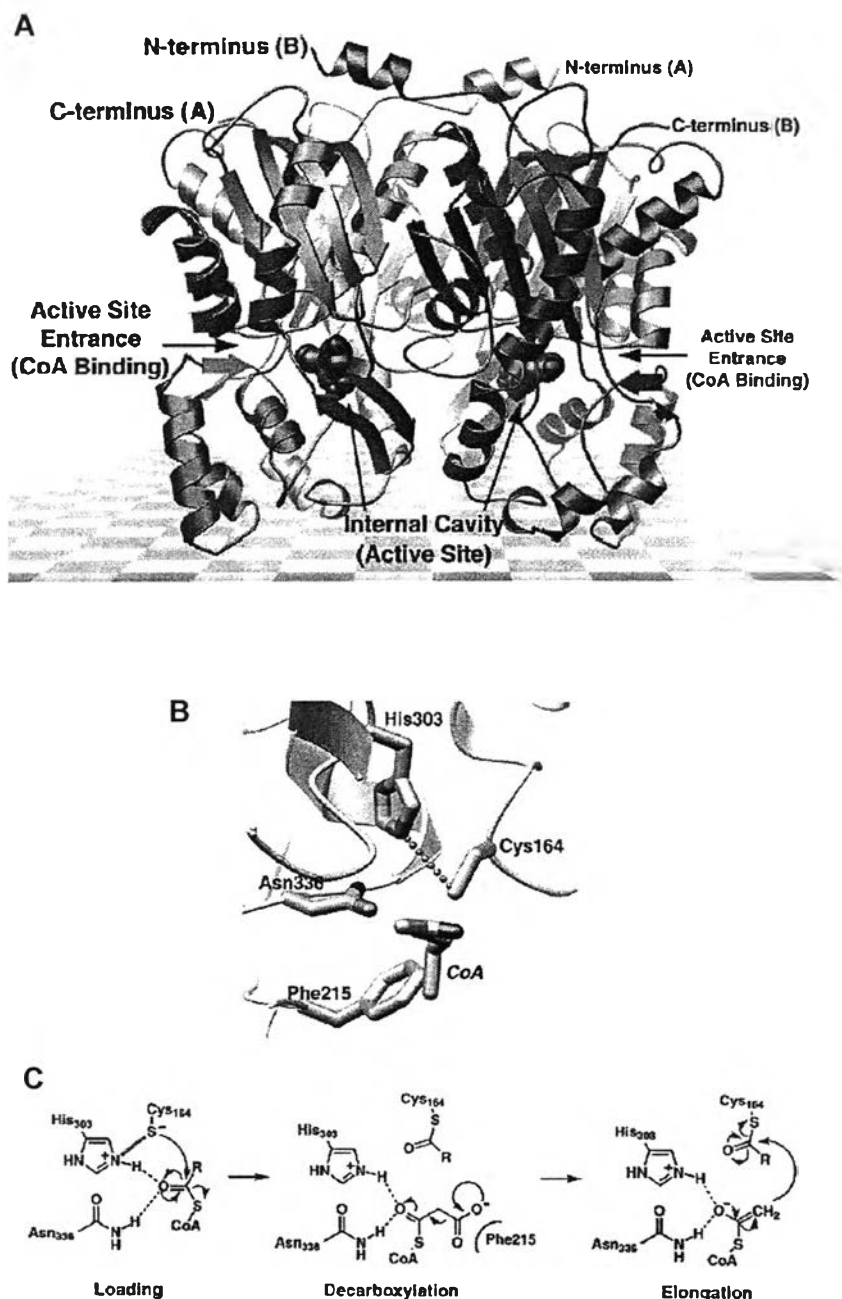


**Figure 6** Structure (A), active site (B) and proposed reaction mechanism (C) of chalcone synthase (CHS). (A) The N- and C-termini for each monomer are indicated. The position of the active site cavity is indicated by the position of the bound naringenin molecule (shown as a space-filling model). The CoA-binding tunnel provides access to the internal cavity. (B) The catalytic residues are shown along with the terminal end of a CoA molecule. The ionic interaction between Cys164 and His303 is indicated by the dotted line. (C) Proposed reaction mechanism of CHS. The loading, decarboxylation, and elongation steps are shown. R is the coumaroyl moiety in the first reaction cycle, coumaroyl-acetyl group in the second cycle, and a coumaroyl-diacetyl group in the final cycle (Ferrer et al., 1999; Jez et al., 2001b).

known CHS- related enzymes (Cys164, Phe215, His303, and Asn336) define the catalytic machinery of CHS as shown in Figure 7. Access to the active site cavity is gained through a 16 °Å -long tunnel that forms the CoA binding site. Structures of CHS complexed with CoA, acetyl-CoA, and hexanoyl-CoA reveal that the panthetheine arm of each ligand extends through the tunnel to position the thioester-linked substrates near the active site cysteine (Ferrer et al., 1999).

Each CHS monomer consists of two structural domains. The upper domain exhibits the  $\alpha\beta\alpha\beta\alpha$  pseudo-symmetric motif observed in fatty acid-ketoacyl synthase. CHS uses a cysteine as a nucleophile in the condensation reaction and shuttles reaction intermediates via CoA thioester-linked molecules or acyl carrier proteins (ACP), respectively. The conserved architecture of the upper domain maintains the three-dimensional position of the catalytic residues of enzyme (Cys164, His303, and Asn336). Structural differences in the lower domain of CHS create a larger active site cavity than that of  $\beta$ -ketoacyl synthase and provide space for the tetraketide required for chalcone formation from *p*-coumaroyl-CoA and three malonyl-CoA. The similar structural features and chemistry of these enzymes imply a common evolutionary origin for the CHS-like enzymes and the ketosynthases involved in fatty acid and polyketide biosynthesis (Ferrer et al., 1999).

### 5.1.2 Mechanism of polyketide formation in CHS

CHS orchestrates the condensation of one *p*-coumaroyl-CoA and three malonyl-CoA molecules into chalcone (Kreuzaler and Hahlbrock, 1975) (Figure 5). Transfer of the *p*-coumaroyl moiety from the CoA-linked starter molecule to Cys164 at the active site initiates the reaction mechanism. Next, the sequential condensation of three acetate units derived from three malonyl-CoA molecules with the enzyme-bound coumaroyl moiety forms a tetraketide intermediate. Inherent in the

	55	58	62	68	98	132	137	164	194	197	206	211	215																																							
Ms_CHS	ELKRF	FD	MCD	SMIRKRYN	ARQDL	VVVEVP	CTLAG	VD	PGA	ENYQQ	DFAGOTVL	VCSEV	AAIFR	HSLSL	QAAGDGAA																																					
Gh_PYS	DLKRF	FD	ICR	SAIKRKYL	ARQDL	VVVEVP	CTLAG	VD	PGA	NLYQQ	DFAGOTVL	VCSEV	AAILFH	HSLSL	QAAGDGAA																																					
Ps_STS	ELKRF	FD	ICR	SAIKRKYL	ARQDL	AMKEVP	CS	TT	PDLPGA	GVFQR	DFAGOTVL	ICSET	AALFR	HSLSL	QAAGDGAC																																					
Bf_BBS	DLKRF	FD	ICR	SAIKRKYL	LRREVA	VVEVP	CTLAG	VD	PGA	NLYQQ	DFAGOTVL	VCAET	TEFFR	HQEDL	QAAGDGAS																																					
Hv_H/EDS	DLKRF	FD	MCD	SMIRKRYN	ARQA	LALVEVP	CTLAG	VD	PGA	ENYQQ	DFAGOTVL	VCSEV	ANAFR	HSLSL	QAAGDGAA																																					
Rg_ACS	ELKRF	FD	ICR	SAIKRKYL	ARQDI	AVVEVP	CS	SAG	VD	PGA	NLYQQ	DFAGOTVL	VCSEV	AALFR	AVSLA	QAAGDGAA																																				
Ha_BPS	ELKRF	FD	ICV	SHIKRKYL	ARQR	ILETEVP	AT	AG	VD	PGA	NLYQQ	DFAGOTVL	VCAEN	AAIFR	HSLSL	QAAGDGAA																																				
Hi_VPS	DLKRF	FD	MCD	SMIRKRYL	TRQDL	VVEVP	CTLAG	VD	PGA	NLYQQ	DFAGOTVL	VCSEV	AAIFR	HSLSL	QAAGDGAS																																					
Hm_CTAS	DLKRF	FD	MCD	SMIRKRYN	GRQDI	VVEVP	CTLAG	VD	PGA	ENYQQ	DFAGOTVL	VCSEV	VINFR	HSLSL	QAAGDGAS																																					
Rp_BAS	NLRQF	FD	ICR	SAIKRKYL	VREKQ	VVEVP	CCLAG	VD	PGA	NLYQQ	DFAGOTVL	VCSEV	TTCFR	HSLSL	QAAGDGAA																																					
	254	256	265	272	293	294	303	308	336	338	375																																									
Ms_CHS	SEGA	D	HLR	T	HL	RDV	GL	G	I	S	D	W	S	I	P	W	I	A	P	G	P	I	L	D	E	Y	G	M	S	A	C	V	L	F	E	N	G	V	L	P	G	F	G	L	T	I	E	T				
Gh_PYS	TEKAV	K	L	HLR	T	Q	H	RDV	GL	G	I	S	D	W	S	I	P	W	I	A	P	G	P	I	L	D	E	Y	G	L	I	S	A	C	V	L	F	E	N	G	V	L	P	G	F	G	L	T	I	E	T	
Ps_STS	SEGA	I	G	HLR	T	Q	K	GAV	DL	G	I	S	D	W	S	I	P	W	I	A	P	G	P	I	L	D	E	Y	G	M	S	A	C	V	L	F	E	N	G	V	L	P	G	F	G	L	T	I	E	T		
Bf_BBS	SARA	T	HLR	H	V	S	KAT	H	RDV	GL	G	I	S	D	W	S	I	P	W	I	A	P	G	P	I	L	D	E	Y	G	M	S	V	C	V	L	F	E	N	G	V	L	P	G	F	G	L	T	I	E	T	
Hv_H/EDS	SEGA	D	HLR	T	HL	RDV	GL	G	I	S	D	W	S	I	P	W	I	A	P	G	P	I	L	D	E	Y	G	M	S	A	S	V	L	F	E	N	G	V	L	P	G	F	G	L	T	I	E	T				
Rg_ACS	SEGA	E	HLR	T	V	R	K	RDV	GL	G	I	S	D	W	S	I	P	W	I	A	P	G	P	I	L	D	E	Y	G	M	S	S	C	V	L	F	E	N	G	V	L	P	G	F	G	L	T	I	E	T		
Ha_BPS	SDGA	T	HLR	S	Y	F	K	EDV	PL	G	V	S	D	W	S	L	P	Y	S	I	P	G	P	I	L	D	E	Y	G	R	G	S	A	C	V	L	F	E	N	G	V	L	P	G	F	G	L	T	I	E	T	
Hi_VPS	SEGA	A	HLR	T	HL	RDV	GL	G	I	S	D	W	S	I	P	W	I	A	P	G	P	I	L	D	E	Y	G	M	S	A	S	V	L	F	E	N	G	V	L	P	G	F	G	L	T	I	E	T				
Hm_CTAS	SEGA	D	HLR	T	H	R	RDV	GL	L	M	S	I	D	S	I	D	W	S	I	P	W	I	A	P	G	P	I	L	E	Y	G	M	S	A	C	V	L	F	E	N	G	V	L	P	G	F	G	L	T	I	E	T
Rp_BAS	SEGA	E	HLR	S	H	Y	RDV	GL	H	I	S	D	W	S	L	P	Y	S	I	P	G	P	I	L	D	E	Y	G	M	S	A	S	V	L	F	E	N	G	V	L	P	G	F	G	L	T	I	E	T			

**Figure 7** Sequence of alfalfa CHS, highlighted in yellow, are aligned against the functional divergent plant type III PKSs. CHS's catalytic triad, residues that contact bound CoA, and other residues important for functional diversity are highlighted in red, green, and blue, respectively. For clarity, only identical residues in the equivalent positions of the aligned sequences are highlighted, even though in some cases conservative substitutions may play an equivalent mechanistic role. Plant sequences: Ms\_CHS, *Medicago sativa* (alfalfa) chalcone synthase; Gh\_PYS (2-PS), *Gerbera hybrida* (daisy) methylpyrone synthase; Ps\_STS, *Pinus sylvestris* (scots pine) pinosylvin-forming stilbene synthase; Bf\_BBS, *Bromheadia finlaysoniana* (orchid) bibenzyl synthase; Hv\_H/EDS, *Hordeum vulgare* subsp. *vulgare* (barley) homoeriodictyol/eriodictyol chalcone synthase; Rg\_ACS, *Ruta graveolens* acridone synthase; Ha\_BPS, *Hypericum androsaemum* (tutsan) benzophenone synthase; Hi\_VPS, *Humulus lupulus* (hop) valerophenone synthase; Hm\_CTAS, *Hydrangea macrophylla* var. *thunbergii* (hydrangea) coumaroyl triacetic acid synthase; Rp\_BAS, *Rheum palmatum* (rhubarb) benzalacetone synthase. (adapted from Austin and Noel, 2003).

condensation reaction is decarboxylation of malonyl-CoA to an acetyl-CoA carbanion that serves as a nucleophile during the chain-elongation reactions. Four amino acids (Cys164, Phe215, His303, and Asn336) situated at the intersection of the CoA-binding tunnel and the active site cavity play essential and distinct roles during malonyl-CoA decarboxylation and chalcone formation (Figure 6B). A series of functional studies focusing on the properties of site-directed mutants of these residues has examined the reaction mechanism of CHS (Lanz et al., 1991; Jez and Noel, 2000; Jez et al., 2000b; Suh et al., 2000).

In the initial loading reaction, the thiolate nucleophile of Cys164 attacks the thioester carbonyl, resulting in transfer of the coumaroyl moiety to the cysteine side chain (Figure 6C, R = coumaroyl) (Lanz et al., 1991; Jez et al., 2000b). The thiolate anion of Cys164 is maintained by an ionic interaction with the imidazolium cation of His303 (Jez and Noel, 2000; Suh et al., 2000). His303 and Asn336 hydrogen-bonded with the thioester carbonyl, further stabilize formation of the tetrahedral reaction intermediate. CoA dissociates from the enzyme, leaving a coumaroyl-thioester at Cys164 (Jez et al., 2001b).

Next, malonyl-CoA binds and positions the bridging carbon of the malonyl moiety near the carbonyl of the enzyme-bound coumaroyl thioester. Asn336 orients the thioester carbonyl of malonyl-CoA near His303 with Phe215 providing a nonpolar bound CoA, and other residues important for functional diversity are highlighted in environment for the terminal carboxylate that facilitates decarboxylation (Jez et al., 2000b). His303 and Asn336 interact with the substrate's thioester carbonyl, creating an efficient electron sink or oxyanion hole that stabilizes the developing negative charge during the decarboxylation step through stabilization of the enol tautomer of the acetyl anion. Moreover, the presence of a stabilized anion also reduces its reactivity toward CO<sub>2</sub>, driving the decarboxylation reaction forward (Jez et al., 2001b).

In the elongation step, attack of the carbanion on the carbonyl of the enzyme-bound coumaroyl thioester releases the thiolate anion of Cys164 and transfers the coumaroyl group to the acetyl moiety of the CoA thioester. Hydrogen bonds from His303 and Asn336 stabilize the tetrahedral transition state of this reaction. Recapture of the elongated coumaroyl-acetyl-diketide-CoA by Cys164 and release of CoA set the stage for two additional rounds of malonyl-CoA decarboxylation and elongation, resulting in formation of the final tetraketide reaction intermediate (Jez et al., 2001b).

The final step in chalcone formation involves an intramolecular Claisen condensation encompassing the three acetate units derived from three malonyl-CoAs. During cyclization, the nucleophilic methylene group nearest the coumaroyl moiety attacks the carbonyl carbon of the thioester linked to Cys164. Ring closure is proposed to proceed through an internal proton transfer from the nucleophilic carbon to the carbonyl oxygen. Breakdown of this tetrahedral intermediate expels the newly cyclized ring system from Cys164. Subsequent aromatization of the trione ring through a second series of facile internal proton transfers yields chalcone (Jez et al., 2001b).

## 5.2 2-Pyrone synthase (2-PS)

A CHS-like enzyme incapable of utilizing *p*-coumaroyl CoA as a starter molecule has been cloned from the ornamental daisy *Gerbera hybrida* (Helariutta et al, 1995). *In vitro*, GCHS2 has been found to synthesize 6-methyl-4-hydroxy-2-pyrone (methylpyrone or triacetic acid lactone (TAL)), by catalyzing two condensations of malonyl-CoA with an acetyl-CoA starter molecule. If acetyl-CoA is not available, the enzyme can decarboxylate malonyl-CoA to make its own acetyl starter, but with ten-fold less efficiency as shown in Figure 8 (Eckermann et al., 1998). Transformation of the daisy with an antisense construct of the *gchs2* gene abolished

the biosynthesis of gerberin and parasorboside, two natural products possessing a reduced methylpyrone scaffold (Figure 8). These glucoside compounds and their derivatives, found in various plant species, are known to inhibit bacterial and fungal growth, and also deter feeding by insects (Eckermann et al., 1998).

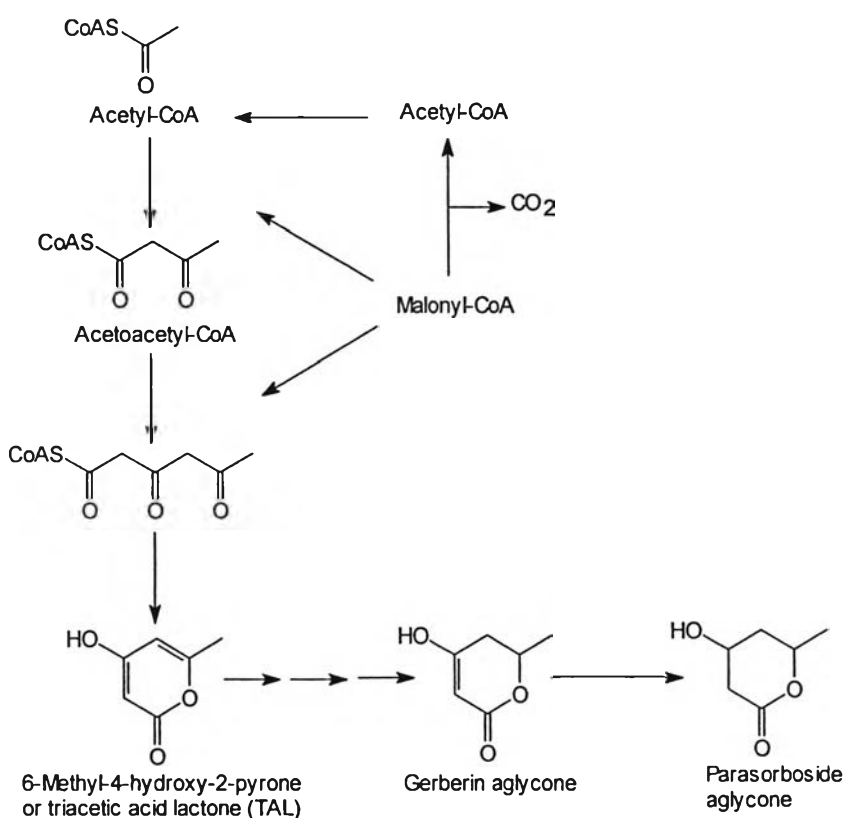


**Figure 8** Reactions of the *Gerbera hybrida* pyrone synthase (2-PS) in the biosynthesis of the aglycone in gerberin and parasorboside. In absence of the starter substrates, the enzyme decarboxylates malonyl-CoA to acetyl-CoA which is then used as starter.

The 2-PS enzyme encoded by the *gchs2* gene has been extensively characterized, yielding new information about the mechanism of functional divergence in type III PKS enzymes. A number of small hydrophobic CoA-thioester starters, including propionyl-CoA, butyryl-CoA, and isovaleryl-CoA, are accepted *in vitro* by 2-PS. Although smaller than the rejected phenylpropanoid starter by only two carbons, benzoyl-CoA is also utilized by 2-PS *in vitro*, undergoing two acetyl additions followed by lactonization to produce 6-phenyl-4-hydroxy-2-pyrone. This latter compound is of interest as a scaffold for a family of HIV-1 protease inhibitors (Eckermann et al., 1998).

Although 2-PS and CHS share 74% amino acid sequence identity (Figure 7), the homology model based on the alfalfa CHS structure has been predicted a smaller active site cavity due to the increased steric bulk of three active site residues, with no other significant changes in structure, despite the hundred or so amino acid differences between CHS and 2-PS (Ferrer et al., 1999). The atomic resolution crystal structure of the *G. hybrida* 2-PS with acetoacetyl-CoA has been determined by using molecular replacement using CHS as a search model (Jez et al., 2000a). The structure has confirmed the validity of the homology model's active site predictions by revealing the active site cavity of 2-PS to possess only a third of the volume observed in CHS. Otherwise, the 2-PS and CHS structures are remarkably similar except for the minor rearrangement of a three-residue solvent-exposed loop at the mouth of the active site, which the 2-PS homology model failed to predict. The resulting interaction of this loop with the adenine ring and phosphates of CoA, as well as other interactions with CoA not observed in CHS, make CoA binding more extensive in 2-PS (Jez et al., 2000a).

However, the mutation of three CHS active site cavity residues to their 2-PS counterparts is sufficient to make alfalfa CHS functionally identical, both in terms of specificity and kinetics, to 2-PS in *in vitro* assays (Jez et al., 2000a). This

CHS triple mutant consists of the following changes at positions that form a triangle in the CHS active site cavity: Thr197Leu, Gly256Leu, and Ser338Ile (Figure 7). An increase in steric bulk at positions 197 and 338 effectively closes off the coumaroyl-binding pocket, excluding large substrates such as phenylpropanoid thioesters, while the increased bulk at the 256 position decreases the size of the putative cyclization lobe of the active site cavity (Jez et al., 2000a). The remarkable functional conversion of CHS into 2-PS by changing less than 1% of their differing residues supports an intuitively simple model of the steric modulation hypothesis, while discounting the relevance of the observed CoA-binding differences to 2-PS's functional divergence from CHS (Austin and Noel, 2003).

While the many differences between the 2-PS and CHS reactions complicate the analysis of this mutagenic conversion, single point mutations of alfalfa CHS at these three positions proved useful in the dissection of their relative contributions to the observed functional differences (Jez et al., 2000a). Not unexpectedly, each of the mutations comprising the triple mutant, when isolated, abrogates CHS's ability to make chalcone. More surprising is the ability of each of the Thr197Leu and Ser338Ile point mutants, but not the Gly256Leu mutant, to catalyze three acetyl extensions of *p*-coumaroyl-CoA. Paradoxically, these changes nearer the putative starter-binding pocket influence the terminating cyclization to a much greater extent than starter molecule specificity. Similarly, all three-point mutants exhibit increased utilization of acetyl-CoA as a starter, relative to wild-type CHS. These results serve as an important reminder of the interconnectedness of specificity for starter usage, chain extension, and cyclization chemistry (Jez et al., 2000a).

### 5.3 Stilbene synthase (STS)

STS enzymes synthesize the same linear tetraketide intermediate (from *p*-coumaroyl-CoA and three malonyl-CoAs) as CHS. However, while CHS cyclizes this intermediate using an intramolecular Claisen condensation between carbons C6 and C1 (Figure 5), STS makes the anti-fungal phytoalexin resveratrol by linking C2 and C7 via an intramolecular aldol condensation, accompanied by an additional decarboxylative loss of the C1 carbon as CO<sub>2</sub> (Tropf et al., 1995) (Figure 9). Resveratrol and related stilbene natural products occur in a limited, yet widely dispersed, subset of the plant kingdom (Tropf et al., 1994).

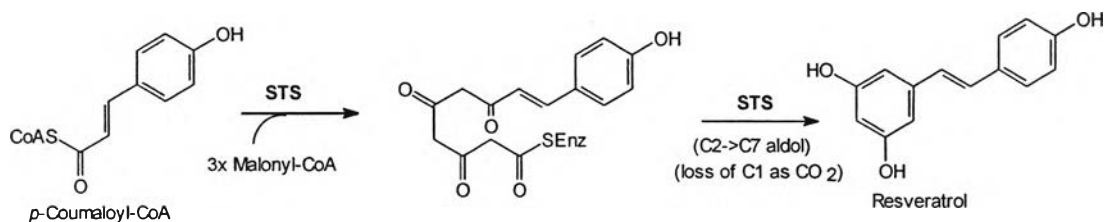


**Figure 9** The formation of resveratrol from *p*-coumaroyl-CoA and malonyl-CoA by stilbene synthase (STS).

The first purification of STS from induced peanut cell cultures in 1984 confirmed that the STS and CHS reactions, although similar, are catalyzed by different enzymes (Schoppner and Kindl, 1984). Cloning and further analysis revealed significant sequence homology between CHS and peanut STS (Schröder, Brown and Schröder, 1988). Apart from the divergent cyclization specificity, no significant mechanistic differences between CHS and STS have been detected (Lanz et al., 1991; Tropf et al., 1995). The subsequent cloning of STSs from pine (Fliegmann et al., 1992) (a gymnosperm) and grapevine (Malchior and Kindl, 1990) (an angiosperm) facilitates a phylogenetic comparison of STS sequences with

each other and with various CHSs, all of which are 60–90% identical at the amino acid level. This study has indicated that STS activity has evolved from CHS on more than one occasion, but failed to identify the STS consensus sequence that could be linked functionally with the mechanistic basis for such divergent cyclization activity (Tropf et al., 1994). In contrast to the case of 2-PS, STS homology models based on the CHS structure reveal no significant differences. Although no evidence for a “steric modulation” explanation for the emergence of aldol cyclization specificity in STS enzymes exists, it has been widely assumed that divergence is achieved through folding of the tetraketide intermediate into an alternative conformation conducive to aldol condensation. Recently, using scaled-up *in vitro* assays and careful analysis of the resultant products, it has been found that both STS and CHS produce small amounts (1-5% of major product yields) of each other’s cyclization product. Additionally, this study demonstrated that STS, like CHS, also generates styrylpyrone side products (Yamaguchi et al., 1999).

Austin and Noel (2003) have determined the crystal structures of both the pinosylvin-forming STS from *P. sylvestris* (pine) and the resveratrol-forming STS from *A. hypogaea* (peanut). Both enzymes, although independently evolved from CHS through different sets of amino acid changes, exhibit similar main-chain conformational changes with respect to CHS. Structure-guided mutagenic conversion of CHS into STS confirmed that STS’s alternative cyclization specificity is achieved by a conformational difference in the main chain of a short, buried loop that spans the dimer interface between the two active sites (residues 132–137) (Figure 7). This movement is caused by various amino acid substitutions at buried positions adjacent to this loop, most notably the replacement of Val98 with a bulkier side-chain, and results in an altered active site hydrogen-bonding network around the slightly repositioned Thr132. This active site residue (conserved in both CHS and STS) changes its bonding interaction with Glu192 (conserved in all type III PKSs), and

forms a hydrogen bond with a well-ordered water molecule adjacent to the catalytic cysteine. A three dimensional comparison of the CHS and STS active sites casts doubt upon models that attribute these enzymes' cyclization differences to alternative productive conformations of their shared linear tetraketide intermediate, achieved by steric differences between the CHS and STS active site cavities. The results suggest instead that subtler active site changes, apparently of an electronic rather than steric nature, favor an alternative cyclization mechanism within the context of a quite similarly folded tetraketide intermediate (Austin and Noel, 2003)

#### 5.4 Bibenzyl synthases (BBS)

A related type III PKS activity is that of the bibenzyl synthases (BBS). These enzymes perform three acetyl elongations of reduced phenylpropanoid starters (dihydrocinnamoyl derivatives), and perform an STS-like (C2->C7) aldol cyclization, resulting in a dihydrostilbene product (Figure 10), leading to dihydrophenanthrenes in orchids (Reienecke and Kindl, 1993).

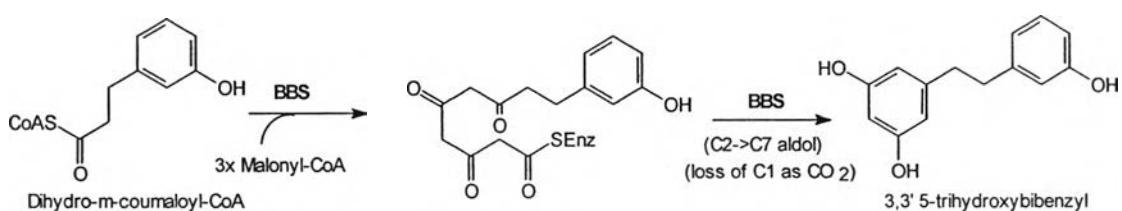


**Figure 10** Reaction of bibenzyl synthase (BBS)

Stressed or wounded orchid tissues, especially those infected by endomycorrhizal fungi, accumulate bibenzyl stilbenes and their tricyclic derivatives, 9,10-dihydrophenanthrenes, presumably as antifungal agents (Gehlart and Kindl, 1991). An enzyme producing the bibenzyl product was purified, characterized, and

subsequently cloned from a *Phalaenopsis* orchid, along with an O-methyltransferase enzyme found to be essential for the further conversion of bibenzyl into 9,10-dihydrophenanthrene (Reienecke and Kindl, 1993; Preisig-Müller, Gnau and Kindl, 1995). This BBS clearly belonged to the CHS/STS superfamily, but preferred dihydro-*m*-coumaroyl-CoA as a starter over *p*-coumaroyl-CoA in *in vitro* assays (Preisig-Müller et al., 1995). Although the steady-state kinetics associated with type III PKS enzymes for their preferred substrates are usually quite similar, BBS's activity towards dihydro-*m*-coumaroyl-CoA is five-fold less than that of STS towards its preferred starter, *p*-coumaroyl-CoA (Preisig-Müller et al., 1997). These starters differ in both the position of ring hydroxylation and in the saturation of their propanoid moiety. Assays using substrate analogues demonstrated that BBS selects for each of these modifications over the more commonly used *p*-coumaroyl starter (Reienecke and Kindl, 1993).

A study utilizing both mutant and BBS/STS chimeric enzymes attempted to elucidate the structural basis for this unusual substrate preference (Preisig-Müller et al., 1997). Chimeras were made by joining the C-terminal portion of grape STS to the N-terminal portion of BBS and *vice versa*, with residue 222 serving as the junction point. Although both chimeras exhibited 50-fold reductions in steady-state activity, the N-terminal segment appeared to dictate starter selection. These authors (in the absence of a three-dimensional structure) also made an STS mutant by replacing STS residues 230–233 with their BBS counterparts. In the context of a 25% loss of resveratrol synthase activity, this mutant exhibited a disproportionate increase in selectivity for the reduced starter. The mutant's rate of conversion of *m*-hydroxyphenylpropionyl-CoA into the bibenzyl product was 11% of its rate of conversion of *p*-coumaroyl-CoA into resveratrol (compared to only 0.35% in wild-type STS) (Preisig-Müller et al., 1997). Notably, these surface-exposed loop residues are

in fact located on the opposite side of the core  $\alpha\beta\alpha\beta\alpha$  domain from the active site, and would seem unlikely to be important for determining specificity. The 25% loss of wild-type activity caused by these changes, which are remote from the active site, suggests that in the context of the STS protein they may be destabilizing to the proper, catalytically active fold (Austin and Noel, 2003).

However, a structure-based examination of the BBS sequence reveals a few residues that might directly influence starter molecule preference (Figure 7). CHS Val98 is replaced in BBS by an alanine, a substitution also found in other divergent type III PKS enzymes known to utilize starters possessing m-substituted phenyl rings. The substitution of CHS Met137 by leucine, also seen in pine STS, may work synergistically with Ala98. A third notable active site feature of BBS is the use of threonine in place of CHS's Gly211. This residue lines the front of the active site cavity, just underneath the gatekeeper phenylalanines located at the end of the CoA-binding tunnel. While this bulky substitution is unlikely to translate into increased specificity for m-substituted phenylpropanoid starters, it presumably changes the shape of BBS's starter-binding pocket. Substrates with reduced propanoid moieties possess increased conformational flexibility, which should give them an advantage over more rigid substrates in binding to a distorted starter-binding pocket. This advantage might be the basis of BBS's selectivity for reduced phenylpropanoid substrates (Austin and Noel, 2003).

### **5.5 Homoeriodictyol/eriodictyol synthase (HEDS or HvCHS)**

In addition to unsubstituted cinnamoyl-CoA and the 4-substituted p-coumaroyl-CoA, plants also commonly produce further substituted phenylpropanoid moieties, primarily used in lignin biosynthesis. These include caffeoyl-CoA, which has hydroxyls at both the 3 and 4 positions, and feruloyl-CoA,

similar to caffeoyl-CoA but O-methylated at the 3 position. Early research showed that CHS could use caffeoyl-CoA as a starter molecule, producing a 3-hydroxylated chalcone (leading to the 3-hydroxylated flavanone eriodictyol) (Saleh et al., 1978). At CHS's optimum in vitro pH of 8, this activity with caffeoyl-CoA is kinetically less favorable than reactions using either *p*-coumaroyl-CoA or cinnamoyl-CoA. Curiously, these same researchers found that the optimal pH for the caffeoyl-CoA reaction is 6.5. At this pH, CHS exhibits nearly equal levels of activity with either substrate (approximately two-thirds of the kinetic efficiency seen at pH 8 with *p*-coumaroyl-CoA). Previously, it was assumed that plants synthesized eriodictyol only via the (post-CHS) 3-hydroxylation of naringenin.

Cloning of an interesting *chs*-like gene (78% amino acid identity with the constitutively expressed barley CHS1) from a library prepared from *Hordeum vulgare* (barley) leaves infected with the fungus *Blumeria graminis* f.sp. *hordei* (*bgh*) (Christensen et al., 1998). Expression of the resulting HvCHS2 enzyme occurs 24–36 h after *bgh* inoculation, corresponding with a 500% increase in the eriodictyol-derived phytoalexin luteonarin. *In vitro*, HvCHS2 was shown to prefer the di-substituted caffeoyl- and feruloyl-CoA starters at physiological pH, with only minimal activity towards *p*-coumaroyl-CoA or cinnamoyl-CoA (Salsh et al., 1978). This unusual substrate specificity is the inverse of that shown by typical CHS enzymes. Activity profiles with all four of these CoA thioesters show that both enzymes exhibit decreasing activity towards substrates that are increasingly different in size from their preferred substrate (*i.e.* too large in CHS1 or too small in HvCHS2) (Christensen et al., 1998). Although HvCHS2 synthesizes pentahydroxychalcone from caffeoyl-CoA and feruloyl-CoA (O-methylated at position 3 when feruloyl-CoA is the starter), the enzyme was labeled a homoeriodictyol/eriodictyol synthase (H/EDS) after the flavanone derivatives of these pentahydroxychalcone natural products as shown in Figure 11.

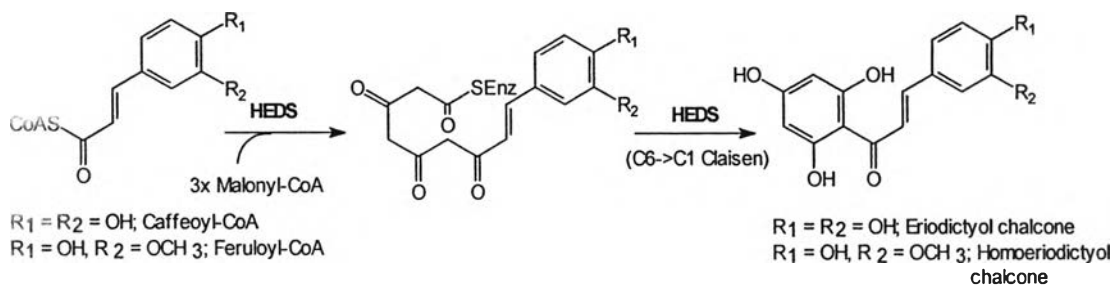


**Figure 11** The formation of homoeriodictyol/eriodictyol chalcone by homoeriodictyol/eriodictyol synthase (HEDS or HvCHS).

Before any type III PKS crystal structure was available, HvCHS2 differed from the CHS consensus sequence, and pointed out three changes that they found particularly notable: Gln95His, Ala166Gly and Gly168Ala (alfalfa CHS numbering) (Christensen et al., 1998). Comparison with the CHS crystal structure, however, reveals two additional and perhaps more functionally important differences (Figure 7). First, substitution in the active site of an alanine for CHS's Thr197 very likely results in the larger starter-binding pocket needed to achieve HvCHS2's unusual specificity for bi-substituted phenylpropanoid-CoA starter molecules. This contrasts with 2-PS's use of a bulkier residue at this same position to decrease the 2-PS active site volume (Jez et al., 2000a). While the Thr197Ala mutation is probably the most relevant change in HvCHS2, other mutations may reinforce the enzyme's preference for larger starters. One likely candidate is a Val98Ala substitution, also observed in other plant type III PKSs that prefer *meta*- and *ortho*-substituted aromatic starter molecules (Austin and Noel, 2003).

## 5.6 Acridone synthase (ACS)

Acridone alkaloids appeared to be restricted to plants of the Rutaceae family (including *Citrus* species). The three-ring acridone skeleton is made by acridone synthase (ACS), a CHS-like enzyme that catalyzes three condensations of malonyl-CoA to an *N*-methylantraniloyl-CoA starter, followed by a CHS-like intramolecular Claisen cyclization of the tetraketide intermediate (Figure 12). Several ACS isozymes have since been cloned from elicited or irradiated cell cultures and from immature flowers (Junghanns et al., 1995; Lukačín et al., 1999; Springob et al., 2000). Although ACS has the unusual characteristic of eluting from gel filtration columns with an apparent molecular weight equal to between one and two monomers, sedimentation equilibrium experiments clearly show the active form to be a homodimer (Lukačín et al., 1999).

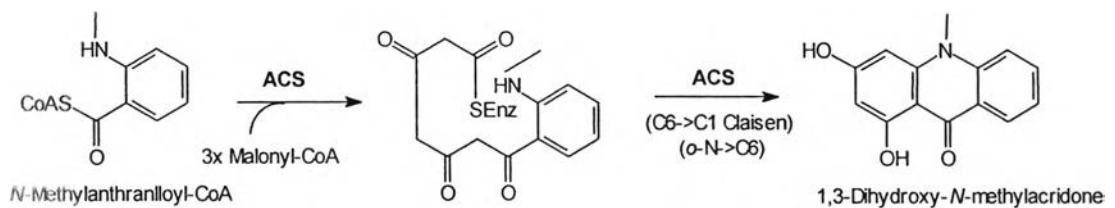


**Figure 12** Reaction of acridone synthase (ACS) from *Ruta graveolens*.

Interestingly, while neither *Ruta* CHS nor any other known CHS or STS can utilize *N*-methylantraniloyl-CoA, wild-type ACS retains some CHS-like activity *in vitro*, producing naringenin chalcone from *p*-coumaroyl-CoA (with about 15% of the activity seen with *N*-methylantraniloyl-CoA) (Springob et al., 2000). Like most divergent plant type III PKSs, the ACS protein sequence differs from CHS in about 100 places. Three of these changes (Thr132Ser, Ser133Ala, and Phe265Val) are in the active site (Figure 7), and were the subject of some recent and enlightening

mutagenesis experiments. Mutation of these three amino acids in the ACS active site to their corresponding CHS residues seriously impaired the mutant ACS's ability to utilize its normal *N*-methylantraniloyl-CoA starter, while greatly increasing CHS like activity towards *p*-coumaroyl-CoA (Lukačín, Schreiner and Mathern, 2001). The corresponding reverse CHS triple mutant has not yet been reported, but the Phe265Val mutation alone does not confer any ACS-like activity on alfalfa CHS (Jez, Bowman and Noel, 2002). When the single mutation of Val265Phe was made in ACS, thus restoring the second CHS gatekeeper phenylalanine, ACS-like activity was impaired, but CHS-like activity did not improve. Clearly, all three changes were important for the evolution of ACS from CHS, but since this ACS triple mutant still possesses marginal ACS-like activity, whereas wildtype CHS does not, additional differences must also be important for allowing the unusually wide *N*-methylantraniloyl-CoA starter into the active site (Lukačín et al., 2001).

### 5.7 Benzophenone synthase (BPS)

Xanthenes are natural products found thus far predominantly in plants of the Gentianaceae and Hypericaceae families. They are formed by a regiospecific ring closure in benzophenone intermediates, which are in turn synthesized by a type III PKS known as benzophenone synthase (BPS). BPS catalyzes three acetyl additions to a 3-hydroxybenzoyl-CoA starter molecule, followed by a CHS-like intramolecular Claisen cyclization and aromatization of the resultant tetraketide intermediate to form 2,3',4,6-tetrahydroxybenzophenone (Figure 13) (Beerhues, 1996). A downstream enzyme, however, rather than BPS, catalyzes the additional, heterocyclic central ring closure to form the xanthone skeleton. Although this downstream enzyme has not been identified, cell culture microsomal assays and inhibition studies indicate that xanthone synthase is a cytochrome P450 oxidase, utilizing an oxidative phenol coupling mechanism (Peter, Schmidt and Beerhues, 1996).

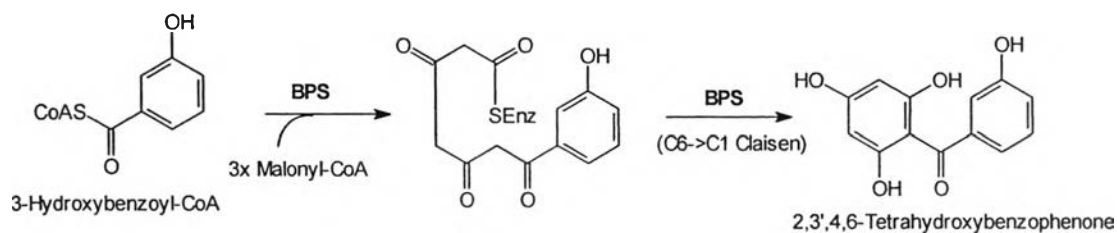


**Figure 13** Reaction of benzophenone synthase (BPS).

Examination of the only BPS sequence deposited in the database (from *Hypericum androsaemum*) reveals a few unusual, yet subtle changes in the active site. Ser338, conserved in most plant type III PKS enzymes that catalyze Claisen or aldol cyclization reactions, is replaced in BPS with a glycine. CHS's second gatekeeper phenylalanine, Phe265, is conservatively mutated in BPS to a tyrosine. CHS's Gly256, known to reduce active site volume when mutated to a bulkier residue (Jez et al., 2000a; 2001a) is a slightly larger alanine in BPS, and finally, position 216, adjacent to the other gatekeeper, Phe215, is occupied by a serine in BPS (Figure 7). The context of the ACS active site, introduction of a bulky side-chain on the buried 216  $\alpha$ -carbon, may translate into a slight decrease in volume of the starter-binding pocket (Austin and Noel, 2003).

### 5.8 Phlorisovalerophenone synthase (VPS)

Bitter acids such as humulone and lupulone are found in the cones of hop plants, which are used by beer brewers to impart a distinctive flavor to this ancient and much celebrated beverage. A divergent type III PKS, expressed in hop cone lupulin glands, was found to synthesize an intermediate leading to biosynthetic elaboration of these important natural products (Zuurbier et al., 1998; Paniego et al., 1999; Okada and Ito, 2001). Phlorisovalerophenone synthase (VPS) accepts either

isovaleryl-CoA or isobutyryl-CoA in an otherwise CHS-like reaction sequence, consisting of three condensations with malonyl-CoA followed by an intramolecular Claisen cyclization to form phlorisovalerophenone or phlorisobutyrophenone, respectively (Figure 14). Interestingly, while CHS enzymes have been shown to accept isovaleryl-CoA *in vitro*, producing a mixture of both phlorisovalerophenone and a triketide-derived lactone truncation product, hop VPS will not accept the CHS coumaroyl-CoA starter (Zuurbier et al., 1998).

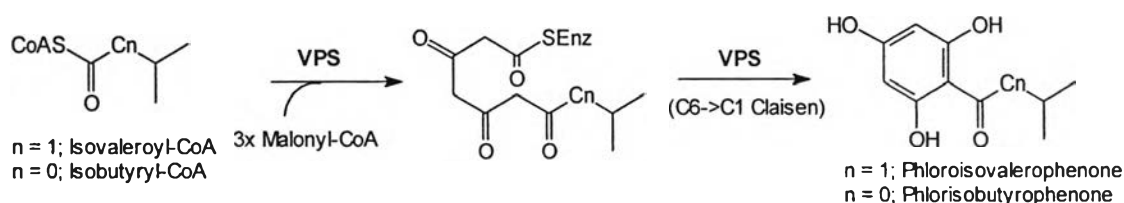


**Figure 14** Reactions of phlorisovalerophenone synthase (VPS)

Comparison of the cloned hop VPS amino acid sequence with the CHS structure reveals a number of interesting differences near the starter-binding pocket. Two active site threonines at positions 132 and 197, conserved in CHS, are replaced with glycine and isoleucine in hops VPS. However, a second VPS has just been discovered in the primitive vascular plant *Psilotum nudum* (Yamazaki et al., 2001). This enzyme uses serines at positions 132 and 197, and a valine at position 338 (Figure 7). The residue at position 338 is a serine in CHSs, hops VPS, and all other plant type III enzymes known to catalyze the CHS-like intramolecular Claisen cyclization (other than BPS). As for the STS reaction, there seems to be multiple active site configurations leading to the VPS reaction. Interestingly, the second-tier Val98Leu mutation that recent work has implicated in the conversion of CHS into STS is also seen in both VPS enzymes (Austin and Noel, 2003).

### 5.9 Coumaroyl triacetic acid synthase (CTAS)

Various species of *Hydrangea* make unusual polyketide natural products. One such compound, hydrangic acid (3,4-dihydroxystilbene-2-carboxylic acid), is a stilbenecarboxylic acid, apparently resulting from an STS-like C2-to-C7 intramolecular cyclization of the typical tetraketide intermediate, but with retention of the C1 carboxyl moiety on the new ring. Another *Hydrangea* product, hydramacroside B, contains a linear tetraketide that could be derived from either the reduced phenylpropanoid dihydro-4-coumaroyl-CoA or from *p*-coumaroyl-CoA (Akiyama et al., 1999). A type III PKS (HmS) has been cloned from *Hydrangea macrophylla* var. *thunbergii* and was shown to produce an uncyclized *p*-coumaroyltriacetic acid (CTA) tetraketide that could be extracted by acidification of the *in vitro* assay mix to form CTA lactone (CTAL) (Figure 15) (Akiyama et al., 1999). These researchers hypothesized that CTAS may catalyze stilbenecarboxylic acid formation *in vivo* when complexed with a hypothetical cyclase. However, both of these *Hydrangea* natural products appear to utilize tetraketide intermediates reduced at the C5 carbonyl; therefore, a ketoreductase (KR or CHR) is the most likely *in vivo* candidate for participation in a CTAS multienzyme complex. Alternatively, the reduction of the linear intermediate itself might be all that is needed to alter cyclization (Akiyama et al., 1999).

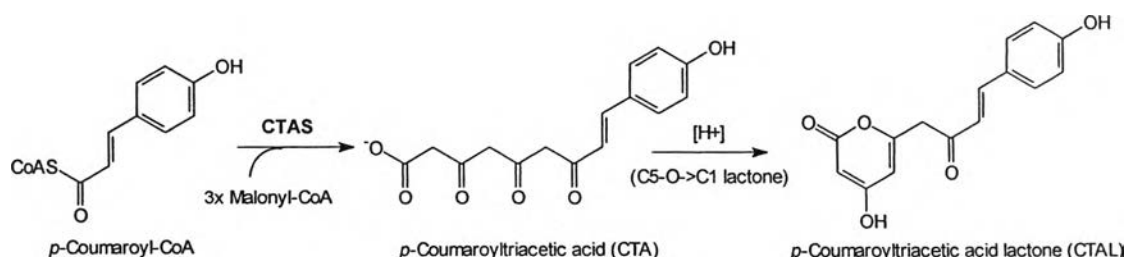


**Figure 15** Reaction of coumaroyl triacetic acid synthase (CTAS).

Sequence analysis of CTAS reveals a substitution in the active site cavity that explains its unusual activity. An asparagine residue replaces the CHS-conserved Thr197 in CTAS (Figure 7). An alfalfa CHS Thr197Leu point mutant was reported to display exactly the same mechanistic phenotype, producing CTAL as a major product when the reaction mixture was acidified (Jez et al., 2000a). Another interesting feature of CTAS is a six-residue insertion (after CHS residue 290) relative to most plant type III PKS enzymes. VPS has four- and two-residue insertions in this solvent-exposed loop on the top of the monomer, remote from the active site. While unlikely to directly affect the mechanistic fate of enzyme-bound intermediates, this insertion is positioned to alter interactions between monomers through proximity to the adjacent and entwined N-terminal helices. In turn, such effects may influence dimerization and/or the formation of (putative) multi-enzyme complexes (Austin and Noel, 2003).

### 5.10 Benzalacetone synthase (BAS)

The characteristic aroma of raspberries is conferred by the presence of *p*-hydroxyphenylbutan-2-one (*p*HPB), also known as the raspberry ketone, whose two-step biosynthesis is initiated by an interesting type III PKS named benzalacetone synthase (BAS) (Borejsza-Wysocki and Hrazdina, 1996). BAS catalyzes a single condensation of malonyl-CoA to the typical *p*-coumaroyl-CoA starter, but then decarboxylates the resulting diketide to form *p*-hydroxyphenylbut-3-ene-2-one (*p*-hydroxybenzalacetone), resulting in the net addition of a single malonate-derived carbon. Next, an NADPH-dependent benzalacetone reductase produces *p*HPB by eliminating the double bond on the linear portion of benzalacetone (Figure 16) (Borejsza-Wysocki and Hrazdina, 1996). BAS has been isolated from raspberries and from rhubarb, where its benzalacetone product is incorporated into the anti-inflammatory glucoside lindleyin (Abe et al., 2001) and may be present in turmeric and ginger as well (Schröder, 1997).

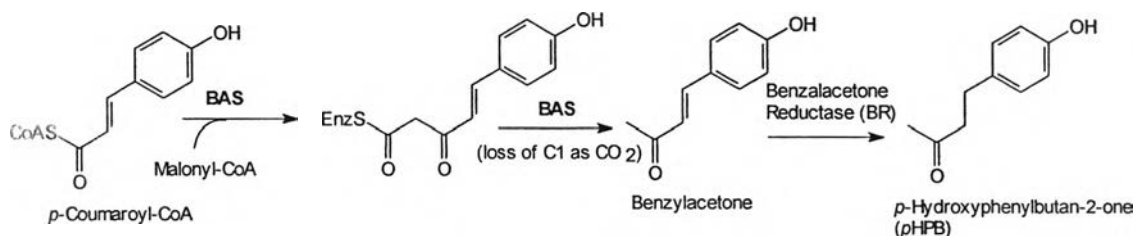


**Figure 16** Reaction of benzalacetone synthase (BAS).

The first purification of BAS from raspberries was complicated by extensive contamination by CHS, but enhanced activity in the presence of either  $\beta$ -mercaptoethanol or ethylene glycol (both inhibit CHS) and a higher affinity for the bulkier feruloyl-CoA than for *p*-coumaroyl-CoA, convinced researchers that the BAS reaction was not merely a derailment of the normal CHS pathway (Borejsza-Wysocki and Hrazdina, 1996). The more recent cloning of BAS from rhubarb (*Rheum palmatum*) revealed its amino acid sequence, and allowed better biochemical characterization after purification from CHS-free *E. coli* expression cultures (Abe et al., 2001). Interestingly, the double bond that is eliminated by the downstream reductase is absent in the hydroxyphenylpropionyl-CoA starters used by the STS-like bibenzyl synthase (BBS) enzymes, but *in vitro*, BAS shows no activity with these reduced starters nor various aliphatic starters accepted *in vitro* by CHS (Abe et al., 2001).

It has been reported to identify a curious substitution in a BAS active site residue when compare with CHS (Abe et al., 2001). Phe215 (alfalfa CHS numbering), absolutely conserved in all other known type III PKS enzymes, is a leucine in BAS (Figure 7). While normally this mutation would be considered conservative, this hydrophobic phenylalanine is proposed to assist in the malonyl decarboxylation and extension reactions, based upon its position in the active site, and conservation and mutational studies (Ferrer et al., 1999; Jez et al., 2000a). However, the presence of a

second unorthodox BAS active site mutation not remarked upon in the literature makes the exact role of the Phe215Leu mutation unclear. CHS's Thr197, sterically altered in a number of divergent type III PKS enzymes, is exchanged for a reactive cysteine in BAS. While no other plant type III PKS uses a second active site cysteine, biosynthetic thiolases use such a cysteine to activate acetyl-CoA by the abstraction of a proton. Perhaps BAS utilizes its second active site cysteine to carry out its unusual decarboxylation of the diketide intermediate. This could involve cleavage of the diketide's thioester bond to CoA (likely to precede the decarboxylation reaction), or donation of a proton to the diketide to facilitate diketide decarboxylation. The nearby Leu215 residue may actively assist in this novel activity, but, conversely, the loss of the conserved gatekeeper phenylalanine might instead only minimize iterative CHS-like elongation of the diketide intermediate, by decreasing the enzyme's more typical decarboxylation activity toward malonyl-CoA, as observed in mutants of CHS Phe215 (Jez et al., 2000a). Regardless of which mechanistic strategy BBS utilizes to execute its unusual reaction, it seems clear that chemical modifications to the type III PKS iterative machinery are involved (Austin and Noel, 2003).

### **5.11 Aloesone synthase (ALS)**

Rhubarb (*Rheum palmatum*, Polygonaceae) is a medicinal plant that produces a variety of aromatic polyketides including chromones, naphthalenes, anthraquinones, phenylbutanones, and stilbenes. Therefore, in addition to regular CHSs involved in the biosynthesis of flavonoids, the presence of functionally different PKSs catalyzing the initial key reactions in the biosynthesis of these metabolites were expected (Abe et al., 2001).

The cloning and characterization of aloesone synthase (ALS), a novel CHS superfamily enzyme that plays a crucial role in the biosynthesis of chromones have been reported (Abe et al., 2004). A cDNA encoding plant type III PKS was cloned from rhubarb. The enzyme accepted acetyl-CoA as a starter, carried out six successive condensations with malonyl-CoA and subsequent cyclization to yield an aromatic heptaketide, aloesone (2-acetyl-7-hydroxy-5-methylchromone) (Figure 17) and shares 60% amino acid sequence identity with chalcone synthases (CHSs) (Abe et al., 2004). In ALS, CHS's Thr197, Gly256, and Ser338, the active site residues lining the initiation/elongation cavity, are uniquely replaced with Ala, Leu, and Thr, respectively. A homology model predicted that the active site architecture of ALS combines a 'horizontally restricting' Gly256Leu substitution with a 'downward expanding' Thr197Ala replacement relative to CHS. Moreover, ALS has an additional buried pocket that extends into the 'floor' of the active site cavity. The steric modulation thus facilitates ALS to utilize the smaller acetyl-CoA starter while providing adequate volume for the additional polyketide chain extensions. In fact, it was demonstrated that CHS-like point mutations at these positions (Ala197Thr, Leu256Gly and Thr338Ser) completely abolished the heptaketide producing activity. Instead, Ala197Thr mutant yielded a pentaketide; 2,7-dihydroxy-5-methylchromone, while Leu256Gly and Thr338Ser just afforded a triketide, triacetic acid lactone. In contrast, Leu256Gly accepted 4-coumaroyl-CoA as starter to efficiently produce a tetraketide, 4-coumaroyltriacetic acid lactone. These results suggested that Gly256 determines starter substrate selectivity, while Thr197 located at the entrance of the buried pocket controls polyketide chain length. Finally, Ser338 in proximity of the catalytic Cys164 guides the linear polyketide intermediate to extend into the pocket, thus leading to formation of the heptaketide in *R. palmatum* ALS (Abe et al., 2006).

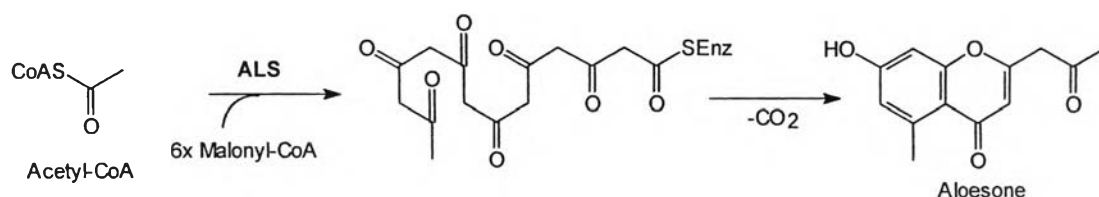


**Figure 17** The formation of aloesone from acetyl-CoA and six molecules of malonyl-CoA by aloesone synthase (ALS).

### 5.12 Pentaketide chromone synthase (PCS)

Aloe (*Aloe arborescens*) is a medicinal plant rich in aromatic polyketides including chromones and anthraquinones. A cDNA encoding the pentaketide chromone synthase (PCS) was cloned and sequenced from young roots of aloe. The enzyme catalyzes formation of a pentaketide chromone, 5,7-dihydroxy-2-methylchromone, from five molecules of malonyl-CoA (Figure 18) and share 50-60% identity to those of CHS-superfamily enzymes from other plants (Abe et al., 2005b). *A. arborescens* PCS maintains an almost identical CoA binding site, and the catalytic triad of Cys164, His303, and Asn336 (in *M. sativa* CHS) is absolutely conserved in all type III PKSs. Furthermore, most of the active site residues including Met137, Gly211, Gly216, Pro375, as well as Phe215 (Austin and Noel, 2003), and Phe265 are conserved in PCS. The CHS-based homology modeling predicted that PCS has the same three-dimensional overall fold as *M. sativa* CHS (Ferrer et al., 1999). The total cavity volume is slightly larger than that of CHS and almost as large as that of *R. palmatum* ALS. One of the characteristic features of *A. arborescens* PCS is that the CHS active-site residues, Thr197, Gly256, and Ser338, are uniquely replaced with Met, Leu, and Val, respectively (Abe et al., 2005b). Interestingly, the three residues are also missing in the heptaketide-forming *R. palmatum* ALS (Thr197Ala/Gly256Leu/Ser338Thr) (Abe et al., 2004; 2006), and in *G. hybrida*

2-pyrone synthase (2PS) (Gly256Leu/Ser338Ile) that also selects acetyl-CoA as a starter to produce a triketide pyrone (Eckermann et al., 1998). A CHS triple mutant (Thr197Leu/Gly256Leu/Ser338Ile) has been shown to yield an enzyme that was functionally identical to 2-PS, suggesting the substitutions are responsible for the starter substrate specificity of the enzymes (Jez et al., 2000a).

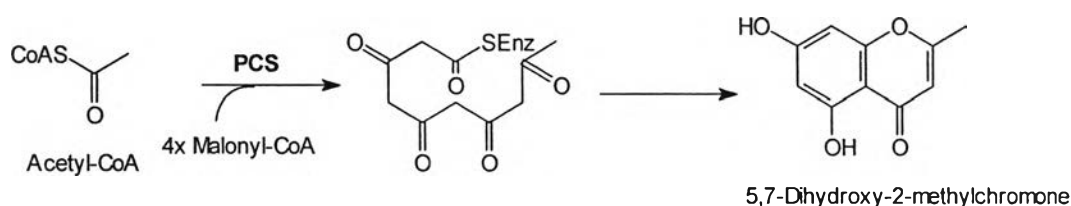


**Figure 18** The formation of 5,7-dihydroxy-2-methylchromone from acetyl-CoA and four molecules of malonyl-CoA by pentaketide chromone synthase (PCS).

### 5.13 Octaketide synthase (OKS)

Octaketide synthase (OKS) is a novel *Aloe arborescences* type III polyketide synthase. The enzyme catalyzed seven successive decarboxylative condensations of malonyl-CoA to yield aromatic octaketides SEK4 and SEK4b, the longest polyketides known to be synthesized by the structurally simple type III PKS (Figure 19) (Abe et al., 2005a). Surprisingly, site-directed mutagenesis revealed that a single residue Gly207 (corresponding to the CHS's active site Thr197) determines the polyketide chain length and product specificity. Small-to-large substitutions (Gly207Ala, Gly207Thr, Gly207Met, Gly207Leu, Gly207Phe, and Gly207Trp) resulted in loss of the octaketide-forming activity and concomitant formation of shorter chain length polyketides (from triketide to heptaketide) including a pentaketide chromone, 2,7-dihydroxy-5-methylchromone, and a hexaketide pyrone, 6-(2,4-dihydroxy-6-methylphenyl)-4-hydroxy-2-pyrone, depending on the size of the side chain (Abe et al., 2005a).

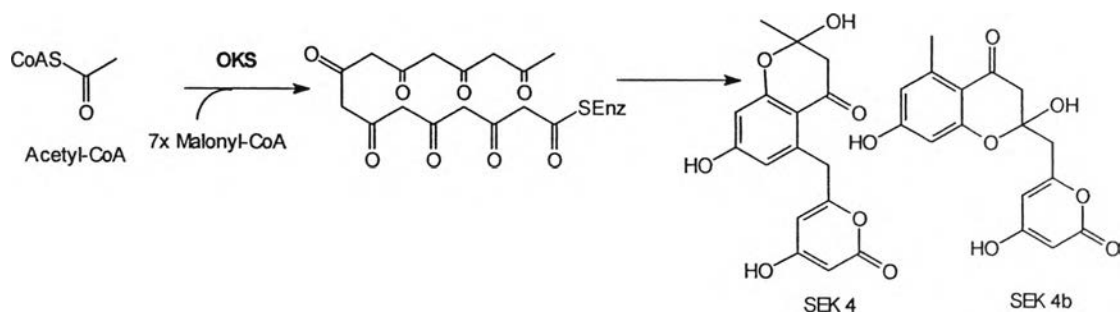


**Figure 19** The formation of SEK4 and SEK4b from acetyl-CoA and seven molecules of malonyl-CoA by octaketide synthase (OKS).